Ocean Engineering 299 (2024) 117409

Contents lists available at ScienceDirect

Ocean Engineering

journal homepage: www.elsevier.com/locate/oceaneng

Time to capsize for damaged passenger ships in adverse weather conditions. A Multi-modal analysis

Francesco Mauro [a,*], Dracos Vassalos [b]

[a] Sharjah Maritime Academy, 180018, Khorfakkan, Sharjah, United Arab Emirates
[b] University of Strathclyde, 100 Montrose St., G4 0LZ Glasgow, Scotland, UK

ARTICLE INFO

Keywords:
Damage stability
Time to capsize
Extreme values
Mixed-Weibull distribution
Collisions

ABSTRACT

After an accident in open seas, the final fate for a damaged ship could be the loss of stability/floatability and consequently capsize/sinkage. The latter may occur even in calm water, but is more critical and probable in adverse weather conditions, i.e., in irregular waves. Identifying a possible capsize event and determining the time that it takes for the ship to capsize is extremely important for safety and risk assessment, meaning whether it would be possible or not to evacuate the ship in a specific scenario and the possibility of loss of life. In this respect, and notwithstanding the impact of many other factors, model tests or time-domain simulations could be used to provide answers to this question. However, even in this case, dealing with irregular waves, entails that both approaches are affected by the random nature of phase spectral components, which leads to a different time to capsize determination at each run/simulation or to the identification of cases where the vessel is not capsizing in the given time window. Here, a dedicated study is provided to describe the time to capsize in irregular waves for critical damages. Simulations performed on a passenger ship at different wave heights and different metacentric heights highlights the appearance of more than one capsize mode for the same damage case. A model based on Mixed-Weibull distributions has been developed to describe the multi-modal behaviour of the time to capsize distributions for the analysed damage cases.

1. Introduction

The damage stability assessment of passenger ships (or ships in general) requires the analysis of the consequences of multiple hazards. Besides standard ship-to-ship collisions, which are included in the SOLAS framework (IMO, 2022), recent enhancements suggest considering also groundings and contacts in the damage stability assessment (Luhmann et al., 2018; Bulian et al., 2020). Such an addition allows for a comprehensive overview of the potential flooding hazards affecting the ship.

However, a thorough damage stability analysis should not be limited to the vulnerability assessment but should include an analysis of risk (Vassalos et al., 2022a, 2023). The concept of risk has been already introduced in the field of damage stability in a set of EU funded and industrial projects (GOALDS, 2012; FLOODSTAND, 2012; Luhmann et al., 2018); however, a proper inclusion of the risk in a complete calculation framework has never been achieved in the past. This was one of the main scopes of the recent EU funded project FLARE 2022. The damage stability framework developed in the EU founded project FLARE 2022 introduces the concept of flooding risk, intending to consider first-principle analyses for the risk evaluation through the determination of the Potential Loss of Lives (PLL). The determination of risk is conceived in a multi-level mode, proposing decreasing levels of approximations for the vulnerability and evacuation analyses (Vassalos et al., 2022b).

To this end, the role of direct simulations is of utmost importance (Mauro et al., 2023) and should not be limited to survivability. A key requirement in the estimation of PLL relates to the evaluation of the Time to Capsize (TTC), which could be estimated only through direct flooding simulations.

In the present work, a novel approach is proposed for the estimation of TTC through a detailed analysis of critical damage cases. It is noted that the diverse capsize modes that may occur in irregular waves for the same damage case leads to a multi-modal behaviour in the resulting TTC distribution. Therefore, a model based on Mixed-Weibull distributions is introduced to describe the TTC, considering the capsize event as a system failure.

The application of Mixed-Weibull distribution to the TTC requires the determination of multiple parameters through a non-linear fitting, here performed with a self-developed method based on a differential evolution algorithm (Mauro and Nabergoj, 2017).

* Corresponding author.
E-mail addresses: Francesco.Mauro@sma.ac.ae (F. Mauro), Dvassalos@sma.ac.ae (D. Vassalos).

https://doi.org/10.1016/j.oceaneng.2024.117409
Received 30 October 2023; Received in revised form 4 March 2024; Accepted 4 March 2024
Available online 5 March 2024

Because an accurate description of TTC requires the execution of a large number of repetitions for each damage case, the proposed approach is suggested for the application to critical cases only, suitably selected with filtering methodologies (Mauro et al., 2022a,b). Here, an example is provided on a critical damage case for a large cruise ship employed for benchmark analyses in project FLARE (Ruponen et al., 2022b). The damage case is reported for four different wave heights and, on the highest wave, for four different values of the metacentric height. The results of the analysis highlight the suitability of the proposed method for the analysis of TTC on critical damage cases, providing the following enhancements to the conventional predictions:

- Determination of distributions for the different capsize modes in a compact format.
- Flexibility in selecting the appropriate statistical value for TTC according to the provided distributions.
- More accurate evaluation of PLL for risk analyses.

To demonstrate the above, the paper first introduces in Section 2 the different capsize modes that may occur in case of a flooding event. Section 3 describes the concept of modelling the capsize as a system failure, presenting the multi-modal approach based on Mixed-Weibull distributions. Subsequently, the reference ship and the reference damage are analysed in Section 4 for different wave heights and metacentric heights. Finally, the implication of the adoption of a multi-modal analysis of TTC in the risk assessment of passenger ships is discussed in Section 5.

2. The capsize of a damaged ship

The most dangerous fate for a ship, in general, and particularly for a passenger ship, is a capsize or sinking event as a consequence of stability/buoyancy loss. As the capsize time is generally short compared to a conventional sinking process, it is extremely important to identify the conditions that may lead to a possible capsize event and potentially reduce or eliminate their occurrence.

2.1. Capsize modes

The identification of a capsize event and the evaluation of the time before this event after a hazard is of utmost importance for the evacuation analysis of the vessel. In fact, in case a damage could potentially lead to the sinking of the vessel, it should be possible to evacuate passenger and crew in less than half an hour. However, capsize may have a different nature, depending on the interaction between floodwater and vessel motions and they are usually identified with the flooding state they relate to.

When the flooding process is studied, the following states can be identified after a hazard:

Transient state : is the first part of the flooding process. The water rapidly inrushes through the breach, causing a rapid heeling into or away from the breach side. The heeling process takes place in a time interval generally shorter than the vessel's natural roll period.

Progressive state : in this state, the water propagates through unprotected flooding paths within the ship, slowly diminishing stability until the vessel sinks, capsizes or reaches a stationary condition. This state may take from minutes to hours, depending on the damage dimension, location and environmental conditions.

Stationary state : in this state, there is no more significant water ingress/egress, the average ship motions are almost constant and a prevalent function of the external loads. The ship may survive or capsize depending on the sea state.

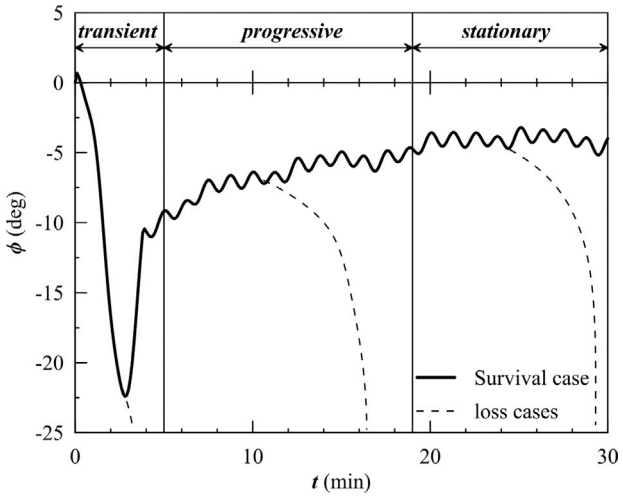

Fig. 1. States of flooding for a damaged ship.

An overview of the above-described flooding states is given in Fig. 1. In case the capsize occurred during the transient phase, the consequences in terms of loss of lives are extreme, as the phenomenon is too fast to even start the evacuation process. When an accident occurred in calm water, then the mechanics of the capsize is only governed by the floodwater progression. In an irregular wave environment, the phenomenon is subject to the randomness of the sea state. In the latter case, it is then not possible to identify a-priori whether the capsize will occur or not in one of the three above-mentioned flooding states.

When a time-domain simulation is performed, a capsize event can easily be recognised from the time history of the roll angle. Thus, when the roll signal exceeds a given threshold (generally above 40 degrees) the vessel is considered to have capsized. However, according to different damage stability frameworks, distinct capsize criteria can be found both for calm water and irregular seas:

Criterion 1: SOLAS heeling failure that considers a maximum heeling of 15 degrees.

Criterion 2: ITTC heeling failure that considers a maximum heeling of 30 degrees.

Criterion 3: ITTC criterion on average heeling that considers an average heeling above 20 degrees in an interval of 3 min.

Criterion 4: cases where the flooding process is still ongoing at the end of the simulation.

The first three criteria refer properly to the roll angle time history, whilst criterion 4 infers that the simulation time is not sufficient to cover the whole flooding process of the selected scenario. Thus, this last criterion is not properly a capsize criterion but could indicate a case where the ship loss may occur with a longer simulation time. In any case, all the above-mentioned criteria do not identify a true capsize, thus when a ship reaches a heeling of ± 180 degrees. Furthermore, a different failure mode can be given by the sinking of the ship, when the vessel lose the whole buoyancy. However, they could be handy for the identification of critical cases for ship safety worthy of being analysed in more detail (Mauro et al., 2022a,b). In the present study, only 'true capsizes' are considered, and, therefore, an alternative methodology is needed to assess the different capsize modes of a passenger ship.

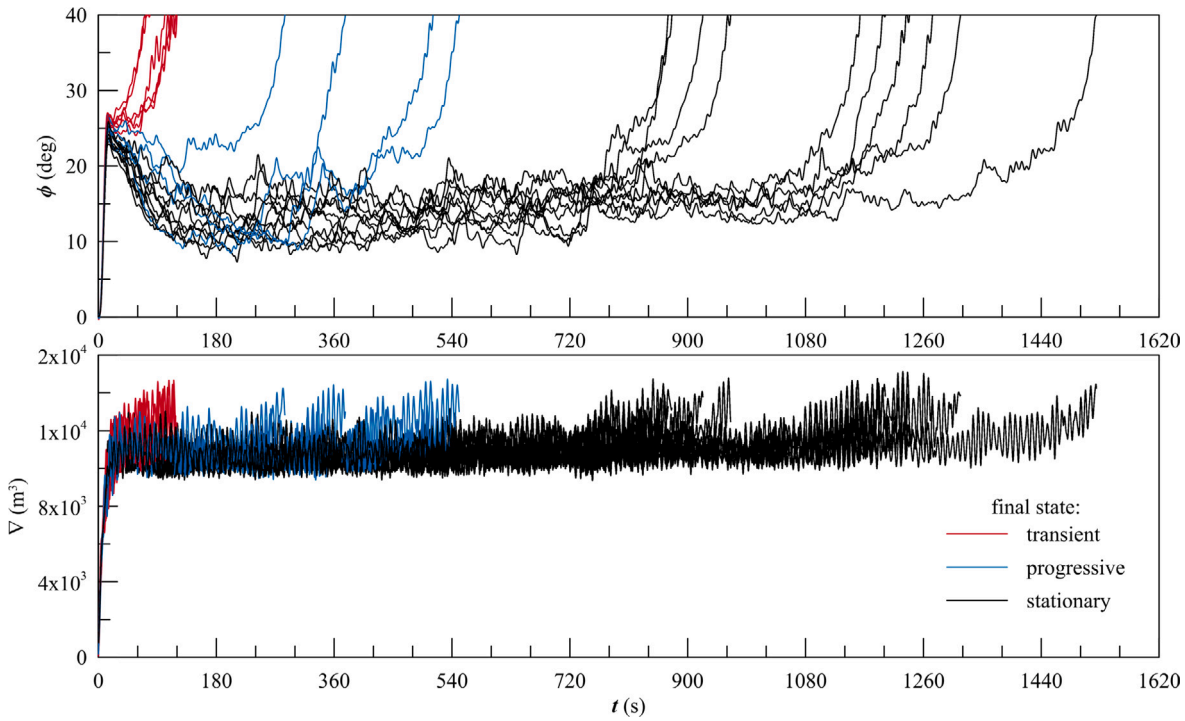

Fig. 2. Roll angle (*top*) and floodwater volume (*bottom*) time traces for 20 repetitions of the same sea state and damage for the FLARE benchmark cruise ship employing the PROTEUS3 solver.

2.2. Time to capsize

When a true capsize is detected, the identification of the Time to Capsize (TTC) is straightforward for the case of calm water, as it is directly extracted from the roll time history of the single simulation:

$$TTC = t_{end} - t_0 \tag{1}$$

where t_{end} is the last time value of the simulation and t_0 is the time corresponding to the beginning of the flooding event. When simulations take place in irregular waves, the TTC is influenced by the randomness of the environment, leading to different TTC results for simulations performed with the same wave parameters (i.e. significant wave height H_s and peak period T_p). As a result, it is common practice to perform multiple repetitions of the same sea state and then use the mean value of the case as a reference for the selected scenario (Cichowicz et al., 2016). In case Monte Carlo simulations are carried out to assess ship survivability, then a cumulative distribution of TTC is found for all damage cases, considering just few repetitions per each damage case in waves (Spanos and Papanikolaou, 2014).

However, a reliable evaluation of the possible risk of loss of lives requires the knowledge of TTC for those critical cases that are worthy of being investigated with evacuation analyses (Vassalos, 2022; Vassalos et al., 2023). Therefore, a more accurate and appropriate procedure for TTC determination should be investigated to be applied only to a restricted number of critical cases.

The conventional approaches to TTC do not consider in detail the nature of the capsizes detected during the time-domain simulations. Furthermore, the relatively small (or excessive) simulation time does not allow for recognising properly reliable distributions for the TTC, justifying the assumption of taking the mean value among the repetitions as significant TTC for further analyses. However, the numerical time-domain simulation codes benchmarking activities within the FLARE project (Ruponen et al., 2022a,b) allow for analysing more in-depth single damage case scenarios, comparing 20 repetitions for a single damage scenario. The results obtained with the PROTEUS3 solver (Jasionowski, 2001) for a cruise ship are shown in Fig. 2, highlighting the different nature of the capsize within 20 repetitions in irregular waves. Nonetheless, also other simulation software highlight the same behaviour for the capsizes (Ruponen et al., 2022b).

From Fig. 2 it is possible to recognise the three different capsize modes described in the previous section. All 20 repetitions end with a capsize; more precisely, 6 are transient, 4 progressive and the remaining 10 are forced oscillation capsize whilst in what was described earlier as stationary state (stationary state capsize mode). The time trace of the roll angle is not helpful to distinguish between progressive and stationary state capsize modes; however, from a direct time-domain simulation (e.g., performed with PROTEUS3 software) it is also possible to monitor the amount of floodwater entering/leaving the ship during the flooding process. Therefore, by analysing the water volume (the bottom graph in Fig. 2) a distinction can be made between progressive and stationary-state capsize modes. Here, an empiric distinction based on the TTC has been made to distinguish between the three capsize modes, namely considering time thresholds. The transient capsize have been considered while occurring in the first 3 min of simulation, the progressive until 12 min and the stationary above this last threshold. This is an arbitrary assumption to give a rough distinction of the three capsize modes as no officially recognised scale is present in literature. As the distinction between the progressive state and the stationary one is purely referred to the test case, no effective real distinction between the cases can be done and it would be preferable to mention the cases as slow-progressive and fast-progressive flooding cases. However, An accurate distinction between the stages can be proposed only in the case a detailed forensic analysis is performed in each specific case, which is a process outside the scope of the paper and is not influencing the findings of the present research.

Furthermore, it is worth noticing that during the benchmark tests, only three repetitions have been carried out (Ruponen et al., 2022b), all resulting, according to the used criterion, in a stationary or, better for the specific case, a slow-progressive capsize.

According to the adopted criterion, the simulations show a net distinction between the three different capsize modes, highlighting a grouping between simulations having similar TTC. Therefore, it is reasonable to assume that the three different capsize modes follow

independent distributions instead of a single one. Such an observation requires a more detailed analysis of the TTC estimation, with a particular emphasis on finding suitable probabilistic distributions that may be used to describe the various phenomena.

3. Modelling capsize as a system failure

Determining suitable distributions to model the TTC is somewhat new topic in damage stability. It is common practice to assume that TTC is associated with a random Gaussian process and consider the mean of multiple repetitions as a significant value for the analyses.

To enhance the perception of TTC, it could be useful to interpret the capsize as a failure of a system (i.e. the damaged ship). This way, it is possible to associate the failure with the commonly used distributions for failure analyses as e.g. Weibull distributions. However, to properly analyse the TTC as a failure, it is handy to define an auxiliary time to capsize TTC* defined as follows:

$$TTC^* = t_{max} - TTC \tag{2}$$

where t_{max} is the maximum allowed simulation time for the damage stability flooding analyses (usually set to 30 min) (Spanos and Papanikolaou, 2014; Vassalos et al., 2022a). Then, it is possible to adopt for TTC* the common representations for failure cases on the Weibull plot, as shown in Fig. 3 for the capsizes reported in Fig. 2. On the Weibull plot, a distribution following a 2-parameter Weibull distribution is identified by a straight line whilst a 3-parameter distribution presents only a concavity or convexity. In the given example of Fig. 3, it is possible to observe that the different capsize modes are not following a single distribution as more than a concave/convexity change is present. Therefore, a more detailed analysis is needed to identify a suitable distribution for TTC*.

3.1. Failure distributions

According to the change of variable identified by Eq. (2), the minimum values of TTC, corresponding to the transient capsize cases, become the maxima of the TTC*. Therefore, with transient capsize cases being the most critical to assess vessel survivability or PLL, it is extremely important to capture such phenomena, thus reproducing with sufficient accuracy the tail of the TTC* population. To this end, the extreme value theory could aid in identifying a suitable distribution for the TTC* description.

As for the multiple repetitions of flooding simulations all capsizes are considered, a proper way to define the capsize event is given by the Fisher–Tippet–Gnedenko theorem (Berliant et al., 1996), stating that the Generalised Extreme value Distribution (GED) should be used to describe the phenomenon under analysis.

GED can be described by the following general cumulative density function:

$$F(x) = \mathrm{e}^{-t(x)} \tag{3}$$

where:

$$t(x) = \begin{cases} (1+\beta z)^{-1/\beta} & \text{if } \beta \neq 0 \\ \mathrm{e}^{-z} & \text{if } \beta = 0 \end{cases} \tag{4}$$

and:

$$z = \frac{x-\gamma}{\eta} \tag{5}$$

The three real constants in Eqs. (4) and (5) are the shape parameter β, defined in $(-\infty, +\infty)$, the scale parameter η, defined in $(0, +\infty)$, and the location parameter γ, defined in $(-\infty, +\infty)$. The shape parameter β value identifies three particular sub-cases of the GED distribution: the Weibull, the Gumbel and the Frechet distributions, respectively. The Gumbel distribution, obtained for $\beta = 0$, defines the extremes of populations, which are supposed to follow an exponential distribution. Frechet distribution (for $\beta > 0$) is used for particular populations

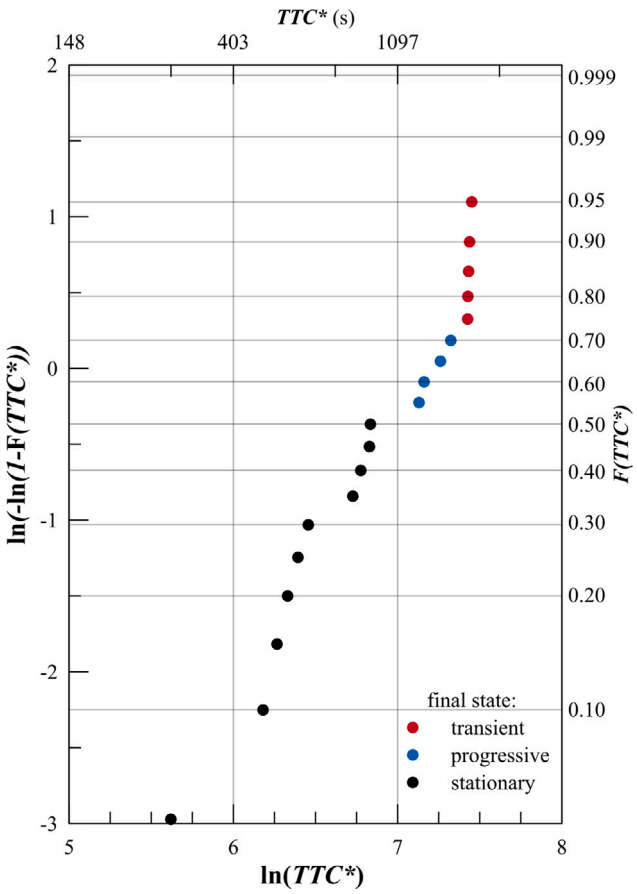

Fig. 3. TTC* representation on the Weibull plot for the FLARE benchmark cruise ship case study.

having a significant amount of data in the tale end (the so-called fat-tale distributions); through a change of sign in the x values. Finally, the reversed Weibull distribution (for $\beta < 0$) represents all the cases not covered by the previous two distributions and is widely used for engineering problems related to defect data analyses in its regular form which implies the use of $\beta > 0$.

Here, Weibull distribution is used as the basis for TTC* analyses. Therefore, it is convenient to rewrite Eq. (3) in the standard cumulative distribution function form adopted for three-parameters Weibull distribution:

$$F(x) = 1 - \mathrm{e}^{-\left(\frac{x-\gamma}{\eta}\right)^{\beta}} \tag{6}$$

Eq. (6) is defined for location parameter values such that $x > \gamma$. However, for particularly complicated cases subject to high levels of non-linearities (Mauro and Nabergoj, 2017), the use of a simple three-parameters Weibull distribution is not enough to represent the data. This is the typical case of multi-modal responses, i.e., sample data that could represent more than one sub-population.

Multi-modal responses may appear for problems characterised by high non-linearities or in failure analyses once a failure can be caused by more than one independent source. This is the case of the capsizing of a ship, where, as previously described, the capsize may have three different modalities, the transient, the progressive and the stationary one, respectively. For such a reason, it is necessary to identify a reliable model capable to describe such non-linear behaviour in the failure modalities. A possible solution could be splitting the record of the capsizes in multiple subsets and directly analysing them with a independent Weibull distributions. However, such a method will intrinsically change the way of sampling of the pecks. In fact, considering some

thresholds in the peaks distribution, makes the hypothesis of the Fisher–Tippet–Gnedenko theorem no more valid. In such a case, the use of a Generalised Pareto Distribution is suggested (Berliant et al., 1996). Furthermore, the process of analysing three different distribution requires the definition of specific thresholds values for the TTC, something that is not available or officially recognised in the literature. Therefore, it is advisable to proceed with a general approach capable of recognising automatically the presence of more than one sub-distribution in the dataset.

A good representation of the multi-modal behaviour of populations could be obtained by employing the so-called Mixed-Weibull distributions. Such distribution is a combination of two or more three-parameters Weibull distributions, resulting in the following cumulative density function:

$$F(x) = 1 - \sum_{i=1}^{N_D} w_i \mathrm{e}^{-\left(\frac{x-\gamma_i}{\eta_i}\right)^{\beta_i}} \tag{7}$$

where N_D is the number of sub-populations and w_i are the percentiles of sub-populations in the total population such that $\sum w_i = 1$. The other parameters are the same as for the three-parameters Weibull distribution defined in Eq. (6).

There are no limitations on N_D but as N_D increases the number of parameters to estimate increases too. For example, fitting a two-sub-population Mixed Weibull distribution requires the estimation of 7 parameters (shape, scale and location parameter for the two distributions plus a single weight factor w), a three-sub-population requires 12 parameters (shape, scale and location parameter for the three sub-populations plus three weights factors w_i) and so on. For such a reason, it is necessary to identify a proper fitting method for the estimation of a high number of parameters.

3.2. Parameter determination

As mentioned above, the fitting of a three sub-population Mixed Weibull distribution requires the determination of 12 parameters. To this end, a methodology based on differential evolution algorithms has been used.

Differential evolution algorithm is an optimisation method employed for multi-dimensional real-valued functions within a population of individual solutions (Storn and Prince, 1997; Mallipeddi et al., 2011). The process does not require the evaluation of gradient function, thus the optimisation problem is not necessarily differentiable. The algorithm investigates the design space using a population of candidate solutions composed of a fixed amount of individuals. At each consecutive iteration, the procedure combines the existing individuals into new candidate solutions. Then, the candidates with the higher ranking for a given objective are kept, so that the new population has a higher score than the previous one. Such a process iterates until a given convergence criterion is satisfied.

The general structure of the optimisation problem is as follows:

$$\begin{aligned} &\min z(\mathbf{x}) \\ &\text{s.t. } g_k(\mathbf{x}) \leq 0 \text{ for } k \in \{1, \ldots, N_c\} \end{aligned} \tag{8}$$

where $\mathbf{x} \in \mathbb{R}^{N_u}$ is the population vector, where each of the N_{POP} (population number) individuals contains an estimate of the N_u unknowns. g_k are the N_c constraints, all function of $\mathbf{x}$. The process includes the possibility of considering both linear and non-linear constraints, as the method does not include the gradient evaluation.

The core steps of the algorithm consist of the process needed to generate the new populations, ensuring the survival of the best members. Considering $\mathbf{x}$ as a candidate solution of the minimisation problem of Eq. (8), at every generation the algorithm forms a mutation vector $\mathbf{v}$ for each $\mathbf{x}$, following the subsequent mutation scheme:

$$\mathbf{v}_i = \mathbf{x}_{r_1} + F\left(\mathbf{x}_{r_3} - \mathbf{x}_{r_2}\right) + F\left(\mathbf{x}_{r_3} - \mathbf{x}_{r_4}\right) \tag{9}$$

where r_1, r_2, r_3 and r_4 are random integer numbers $\in [1, N_{POP}]$, distinct and other than i. F is a real scale parameter varying in $[0, 2]$, small values of F generates low mutation of elements, large values of F are suitable for wide investigations along the possible solutions space.

After the mutation process, the algorithm creates an auxiliary vector $\mathbf{t}_i$ using either elements of $\mathbf{x}_i$ and $\mathbf{v}_i$ adopting the following crossover procedure on each element of $\mathbf{x}_i$ and $\mathbf{v}_i$:

$$t_{i,j} = \begin{cases} v_{i,j} & \text{if } s_{i,j} \leq p_c \\ x_{i,j} & \text{otherwise} \end{cases} \tag{10}$$

where $i = \{1, \ldots, N_{POP}\}$, $j = \{1, \ldots, N_u\}$, $s_{i,j}$ is a uniformly distributed random number in [0,1] and $p_c \in [0, 1]$ is the crossover probability.

After the crossover process, the algorithm calculates the objective function z for $\mathbf{t}$ and compares $z(\mathbf{t}_i)$ with $z(\mathbf{x}_i)$. In case $z(\mathbf{t}_i) < z(\mathbf{x}_i)$, then $z(\mathbf{t}_i)$ replaces $z(\mathbf{x}_i)$. Such a process ensures that the new population is a mix of the better elements of the old population and the new individuals.

The process requires the user to provide only three parameters: the population number N_{POP}, the scale factor F and the crossover probability p_c. Additional parameters could be added to provide constraints concerning the limitation to the parameters values or stopping criteria for the objective function evaluation. Therefore, the method can be easily applied to various optimisation problems, including the data fitting of a mixed function.

For fitting problems, the objective function should represent the quality of fitting. For such a reason, in the present work use has been made of the determination coefficient R^2, calculated in the following way:

$$R^2 = 1 - \frac{SS_{res}}{SS_{tot}} \tag{11}$$

where:

$$\begin{cases} SS_{res} = \sum_{i=1}^{N_p} \left(y_i - f_i(\mathbf{x})\right)^2 \\ SS_{tot} = \sum_{i=1}^{N_p} \left(y_i - \bar{y}\right)^2 \\ \bar{y} = \frac{1}{N_p} \sum_{i=1}^{N_p} y_i \end{cases} \tag{12}$$

where y_i are the N_p record data point, $\bar{y}$ is the mean value of the data and f_i are the fitted value coming from the reference equations at the same point. As the optimisation problem provided in Eq. (8) is a minimisation and the objective of the fitting is maximise R^2, the effective objective function of the problem is $-R^2$.

The algorithm has been already tested and compared against other methods for data fitting (Mauro and Nabergoj, 2017), highlighting its equivalence to least mean square, log-likelihood and moments method for the fit of extreme value distributions, providing the capabilities to work with mixture distributions like the three-sub-populations Weibull. According to the previous studies on such kind of problems, the most adequate parameters set to use for the algorithm are $N_{POP} = 8N_u$, $F = 1.1$ and $p_c = 0.9$. Such values have been utilised for all the regression analyses performed during the present investigation.

4. Application on a cruise ship

The developed analyses described in the previous sections are applied here on a reference case employed through several studies in the FLARE project. The test case refers to a large passenger ship (more precisely a cruise vessel) having the general arrangement shown in Fig. 4 and the main particulars given in Table 1. The vessel is the same employed for the benchmark studies (Ruponen et al., 2022b) and advanced investigations on first-principles-based damage stability frameworks (Mauro et al., 2022a,b).

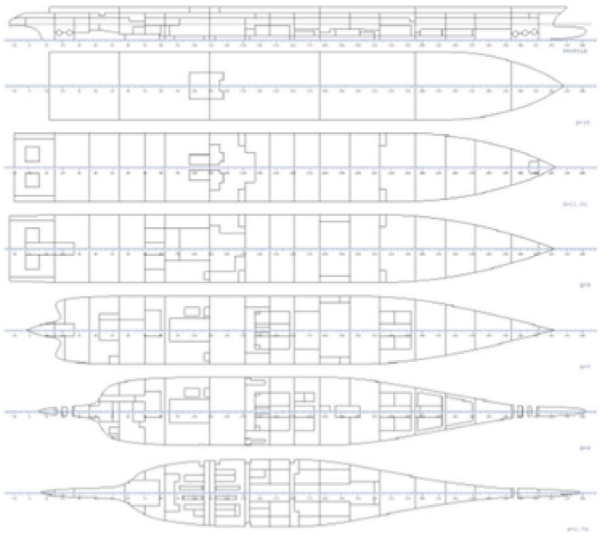

Fig. 4. General arrangement of the reference cruise ship.

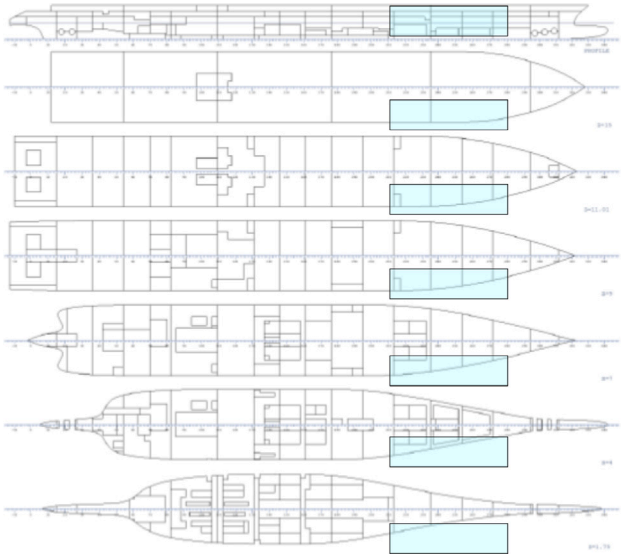

Fig. 5. Longitudinal and horizontal view of the reference damage breach.

Table 1
Main characteristics of the reference passenger ship.

Parameter	Symbol	Value	Unit
Length overall	L_{OA}	300.0	m
Length between perpendiculars	L_{PP}	270.0	m
Beam	B	35.2	m
Subdivision draught	T	8.2	m
Height at main deck	D	11.0	m
Deadweight	DWT	8000	t
Gross tonnage	GT	95 900	–
Number of passengers	N_P	2750	–
Number of crew members	N_C	1000	–

4.1. Reference damage case

To apply the TTC analyses, a reference damage case has been selected, the same as the benchmark tests, the results of which are shown in Figs. 2 and 3 for the time traces of roll and Weibull plot, respectively. However, the ship model employed for the benchmark study refers to a simplified internal layout of the vessel. Here, to address a more realistic case, the full compartmentation of the vessel is used, as it is represented in Fig. 4. Such an internal subdivision follows the guidelines for time-domain flooding simulations established and consolidated within the project FLARE (Guarin et al., 2021).

Table 2
Environmental and GM values for the case study.

Test ID	H_s (m)	T_p (s)	GM (m)
TEST-1	3.50	5.965	2.870
TEST-2	3.75	6.174	2.870
TEST-3	4.00	6.377	2.870
TEST-4	4.25	6.573	2.870
TEST-5	4.25	6.573	2.895
TEST-6	4.25	6.573	2.920
TEST-7	4.25	6.573	2.970

The selected breach damage has a length of 44.2 m, a penetration of 10.0 m, a height of 16.0 m starting from a lower vertical limit of 0.0 m. Fig. 5 provides an overview of the breach location and dimensions on the longitudinal view of the reference ship. The damage is representative of a significantly large and critical damage for the reference ship, resulting from a preliminary set of calculations. This preliminary screening of simulations represents a stress test for the ship, including only damages with the maximum allowable damage length by SOLAS and severe sea states with a significant wave height $H_s = 7.0$ metres (Vassalos and Paterson, 2021).

The present study does not consider the 7.0 metres wave height, this being not realistic as an operational scenario and also outside the reliability bounds of the flooding simulation code employed during this investigation. Instead, four different wave heights have been investigated, starting from 3.50 to 4.25 metres in step of 0.25 m. Furthermore, different conditions for the metacentric height GM have been tested for the $H_s = 4.25$ m, considering the initial GM of 2.870 metres and increasing it up to 2.970 metres. Table 2 reports a comprehensive list of the tests performed in this study with the associated conditions.

4.2. TTC analyses

The reference damage case consists of simulations having a maximum time of 30 min, as suggested by old and recent studies in damage stability (Spanos and Papanikolaou, 2014; Guarin et al., 2021; Mauro et al., 2023). All the simulations led to the vessel capsize within the simulation time. Therefore, the resulting set of 100 capsizes per test case represents a suitable population for the fitting methodology described in the previous section.

It is advisable to check the goodness of fit through conventional estimators. In this case, use has been made of the R^2 and R^2_{adj} coefficients, defined as per equation (11) and as follows:

$$R^2_{adj} = 1 - \left(1 - R^2\right) \frac{n-1}{n-n_p-1} \tag{13}$$

For evaluating R^2_{adj}, the number of predictors of the regression model n_p needs to be provided. Through these two coefficients it is possible to determine the quality of the proposed regression models.

The following subsections describe the results of the multi-modal analyses for the cases at constant GM and variable H_s and for the variable GM at constant H_s, respectively.

4.2.1. Constant GM and varying H_s

The first set of calculations refers to the cases with constant GM and different significant wave heights H_s, corresponding to the tests from 1 to 4 according to the nomenclature provided in Table 2. For each test 100 simulations have been carried out with PROTEUS3 software in irregular waves, considering a JONSWAP (Hasselmann and Olbers, 1973) spectrum with an elongation parameter $\gamma_J = 3.3$, a constant wave steepness of 0.2 and significant wave heights varying from 3.50 to 4.25 metres, in steps of 0.25 metres. The software PROTEUS 3 is based on the resolution of 4DOF rigid-body ship motion equations

(neglecting surge and yaw), coupled with the floodwater dynamics. The flooding process is governed by the Bernoulli's equation, while the water inside compartment is modelled as a lumped mass. Froude–Krylov and restoring forces are integrated up to the instantaneous wave elevation both for regular and irregular waves. Radiation and diffraction forces are derived from 2D strip theory calculations. Hydrodynamic coefficients vary with the attitude of the ship during the flooding process (heave, hell and trim). The vessel is assumed free to drift, with drift forces evaluated by empirical formulations. The simulations considers only the damaged ship, without considering the presence of a striking ship in the simulations. The model used for the calculations is including corridors and staircases connected one to each other by relevant openings to allow the progression of flooding across and in-between adjacent decks. As an assumption, for the simulations, all the openings have been considered opened.

The time to capsize has been derived for all the simulations, evaluating TTC* according to Eq. (2). To present the results it is convenient to adopt a representation on the Weibull plot, where the x-axis presents the $\ln TTC^*$ and the y-axis reports $\ln(-\ln(1-F(TTC^*)))$. For this particular plot, the Weibull distribution with 2 parameters (neglecting the location parameter γ) is represented by a straight line, while the 3 parameters distribution present a concavity or a convexity according to the sign of γ.

Fig. 6 presents the results for the four test cases on the Weibull plot. The Figure reports the TTC* distributions together with the fitting obtained with the Mixed Weibull models. The distributions highlight the same behaviour noticed for the benchmark test case performed in FLARE project and already reported in Fig. 3. Even though the fitting obtained by applying the differential evolution algorithm seems to capture the population's behaviour well, it was thought appropriate to check the goodness of fit through conventional estimators. As mentioned above, use is made of R^2 and R^2_{adj} evaluated according to Eqs. (11) and (13), respectively. Employing the above indicators makes it possible to evaluate the quality of the proposed regression model. Table 3 gives the obtained regression parameters and the goodness of fit indicators, where it is possible to observe the quality of the regressions.

For all the four tested cases, both R^2 and R^2_{adj} are above 0.99, highlighting the good quality of the obtained regression models. The values shown in the table allow for a more accurate description of the distributions that characterise the different capsize modes. The location parameter γ allows for identifying the capsize type. High values of γ refer to the transient capsize as high TTC* corresponds to a low TTC value according to Eq. (2). The scale parameter η does not add additional considerations for the characterisation of the capsize event. On the other hand, the shape parameter β identifies how the capsizes are distributed along TTC*.

The transient capsizes present a high β value, which means that they are all distributed along a short TTC* interval. The progressive and stationary capsize distribution present a different shape compared to the transient as they cover a wider interval of TTC*. As an example, considering the case with $H_s = 3.75$ m (TEST-2), the shape parameter for the stationary case is close to 2, which means it is similar to a Rayleigh distribution. For the same wave height, the progressive case has a β value close to 5, which means that it follows a general Weibull case. For all the other tests, the shape parameters for progressive and stationary state are all between 0.9 and 2.0, so varying from shapes close to exponential distribution up to a Rayleigh case. For such a reason, the selection of a Weibull model for the modelling grants sufficient flexibility to capture the behaviour of the capsize modes.

Fig. 7 shows the cumulative density functions of the individual distributions for transient, progressive, and stationary state capsizes, together with the Mixed-Weibull one. From this picture, all the aforementioned considerations can be easily visualised. The figure highlights the different progressive and stationary capsize behaviour between the four different wave heights tested.

However, by changing the significant wave height, the nature of the distributions for progressive and stationary capsize also vary, suggesting that the general Weibull model is appropriate to cover the possible distributions of the different capsize modes. Adopting simpler distributions commonly used in naval architecture, such as Rayleigh or exponential models, may lead to appropriate fitting only in some particular cases.

A final consideration relates to the weighting factors w. From Table 3 it can be observed that the contributions of the stationary and progressive sub-distributions to the final Mixed Weibull are always between 0.34 and 0.46, while the transient contribution attests from 0.13 to 0.22, depending on the single cases. This means that there is not a unique trend between the w factors and the wave heights for the provided test case, but that the contributions remains almost constant between the tests.

4.2.2. Constant H_s and varying GM

A second set of tests has been carried out at constant H_s and varying the metacentric height GM. The aim of this set of tests is studying the effect of the changes in GM on the distributions of capsizes, with a particular interest to the distribution of the transient capsize case. The tests have been performed for the higher significant wave height considered in the previous set of calculations (4.25 m). The same number of repetitions and the same settings for the environmental conditions have been applied. Fig. 8 shows the Weibull plot for the additional test cases TEST-5, TEST-6 and TEST-7, reporting also TEST-4 to have a complete overview of the effect of GM change for the case with $H_s = 4.5$ metres. For the tests at higher GM, the calculation time of the simulation has been increased to 1 h of simulation to detect all the cases of stationary state capsize.

From the figure, it is evident how the increasing value in GM changes the outcome of the damage simulations. Despite all the cases leading to a final capsize, compared to TEST-4 the transient cases diminished in amount for TEST-5 and disappear in TEST-6 and TEST-7. Also in this case, the fitting curves highlight a good reproduction of the simulated distributions of TTC*. As a confirmation, Table 4 shows the R^2 and R^2_{adj} values for the different GM tests, all above 0.99.

The Table shows also the regression coefficients of the Mixed distribution. As for the previous case, the location parameter γ identifies clearly the distributions of stationary, progressive and transient capsize. High value of γ corresponds to the transient case, while the lowest is for the stationary case. Same considerations as for the previous tests concern the shape parameter β, ranging from the identification of an exponential distribution up to more generic Weibull shapes, especially for the transient capsize. Relevant is the interpretation of the weights w. As mentioned, the transient cases disappears as GM increases; however, the differential evolution algorithm fits always three sub-populations. Analysing the weighting factor, it is possible to observe that the weight of the transient distribution drops down up to be almost equal to zero for the higher GM cases.

For such a reason, the fitting algorithm is powerful as with a single model could intrinsically capture also cases when only 2 sub-populations are relevant to the modelling, like in TEST-6 and TEST-8. Such a characteristics can be observed also in Fig. 9, where the cumulative density functions of the tested case are shown. For TEST-4 and 5, the transient distribution has an impact on the final cumulative function, but for TEST-6 and 7 the contribution is negligible. Such a matter further highlights the high fitting capability of the implemented differential evolution algorithm.

4.3. Concluding remarks

The previous sections presented the output of the Mixed Weibull distribution fitting process on the test cases with varying H_s or varying GM. The possibility to identify the single distributions of stationary, progressive and transient capsize is an added value to the forensic

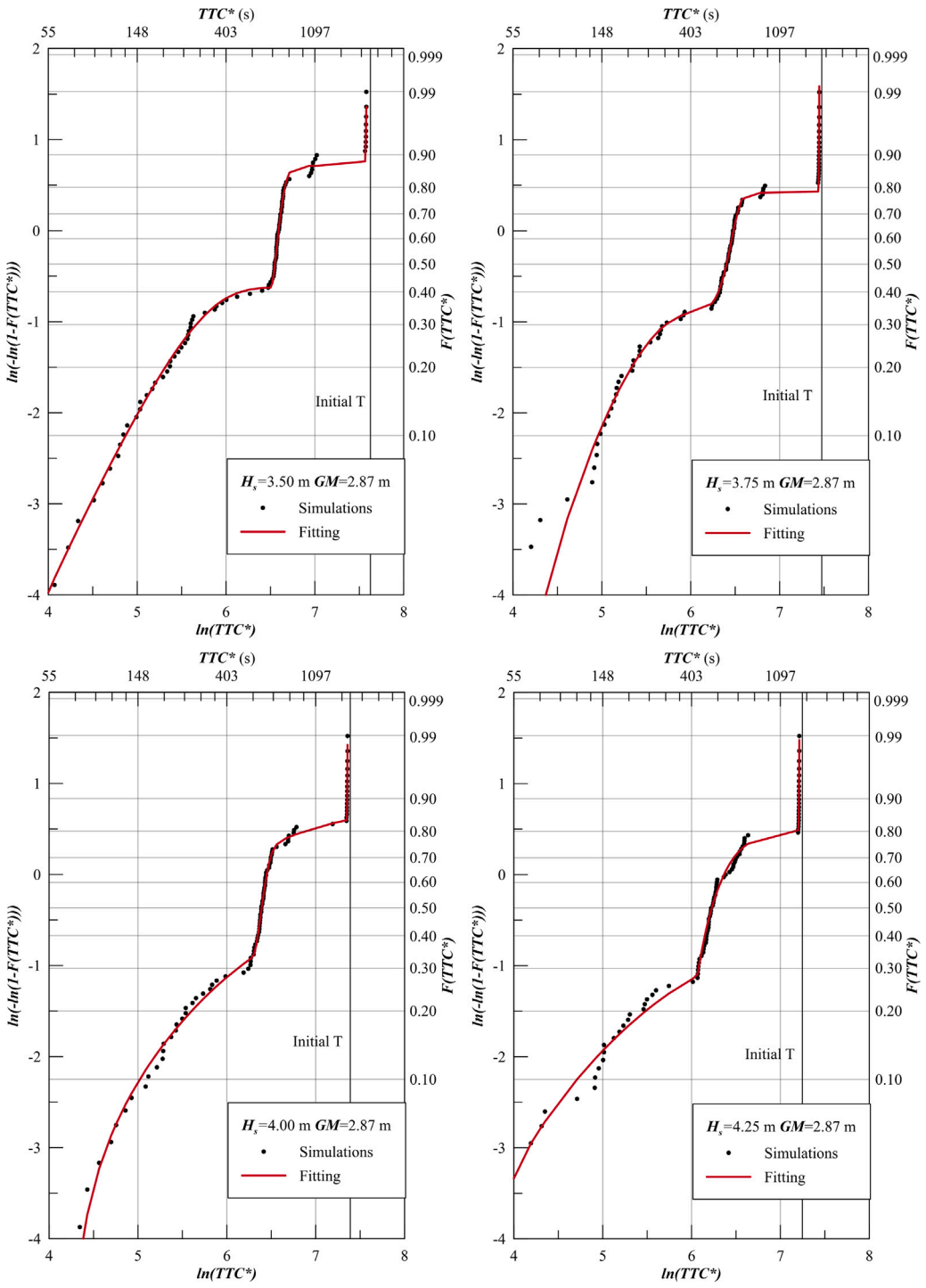

Fig. 6. TTC* cumulative distribution function and Mixed Weibull fitting on the Weibull plot for the reference damage case in TEST-1 (*top-left*), TEST-2 (*top-right*), TEST-3 (*bottom-left*) and TEST-4 (*bottom-right*).

analysis of critical damage cases leading to capsize. The possibility to have a model that covers all the distributions allows for evaluating more in detail which is a suitable value for the consideration of the TTC, necessary to compare with evacuation analyses.

The most recent frameworks for damage stability considers only the mean value of 5 repetitions as the significant value for the TTC (Vassalos et al., 2022a). Such an assumption is not taking into account the possible extreme events that may occur in the reference damage case, i.e. the transient capsize. In fact, defining the cumulative density function of the TTC* distribution it is possible to consider the extreme value for TTC*, and, consequently, evaluate the extreme TTC events leading to transient capsize. Such a methodology, allows for considering statistically significant events like the 0.98 percentile, relevant to establish extreme events (Mauro and Nabergoj, 2017). Table 5 reports the mean values and the percentiles values of all the tested cases. It is evident that the difference is extremely high, especially for cases where the transient capsize are considerably height.

The identification of the percentile can be done by direct interpolation of the cumulative curve, as it is not possible to invert the final formulation of the Mixed Weibull distribution. Inversion process requires the adoption of simpler formulations. Table 5 reports also the mean of the first 5 consecutive repetitions, value usually adopted by

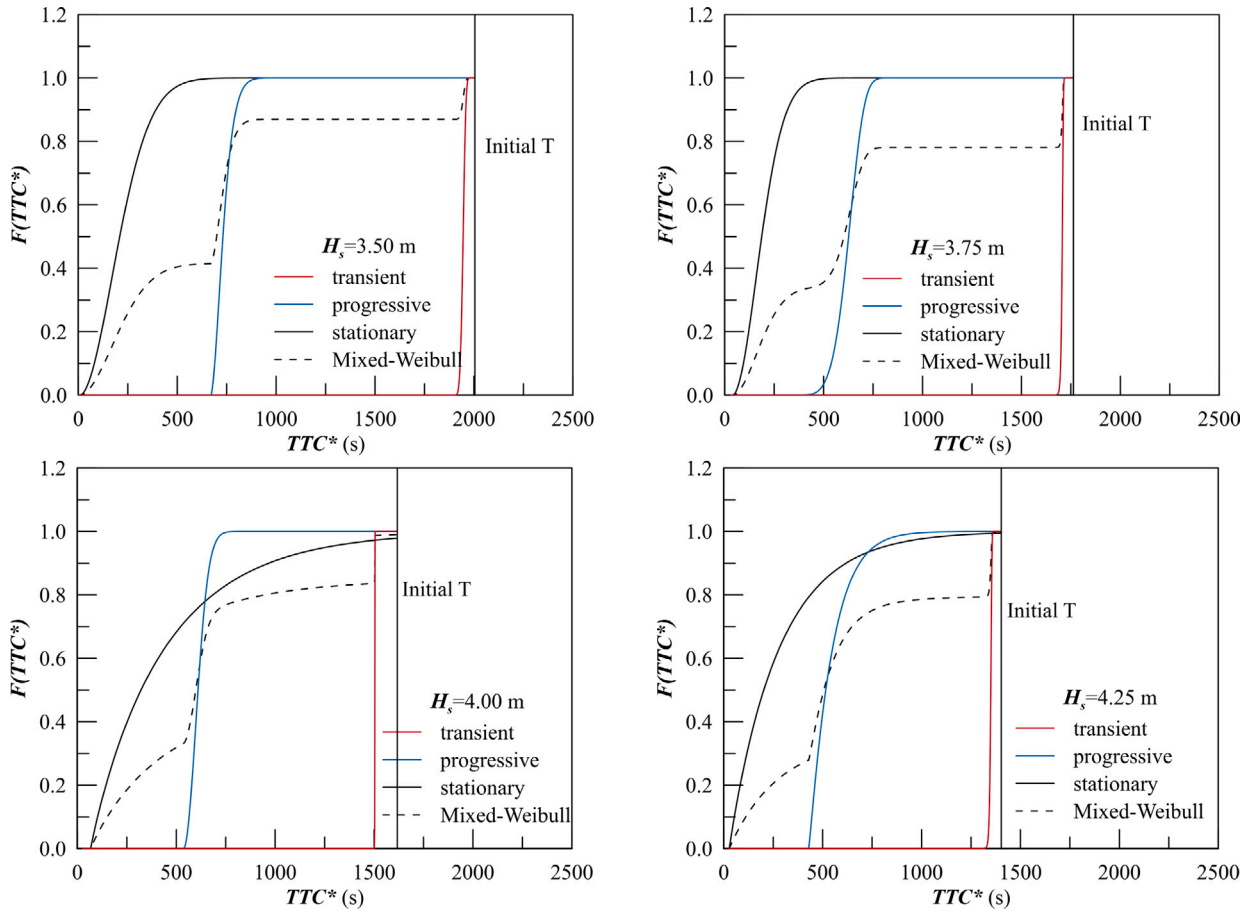

Fig. 7. Cumulative distribution functions for the transient, progressive and stationary capsize for TEST-1 (*top-left*), TEST-2 (*top-right*), TEST-3 (*bottom-left*) and TEST-4 (*bottom-right*).

Table 3
Best fitting parameters for the Mixed Weibull distribution on the reference damage case with constant GM and varying H_s.

Test	Tmax	Distribution	η	β	γ	w	R^2	R^2_{adj}
TEST-1	2005.16 s	stationary	245.871	1.862	7.367	0.415	0.9984	0.9982
		progressive	75.971	1.617	670.429	0.455		
		transient	48.998	4.588	1900.001	0.130		
TEST-2	1762.77 s	stationary	178.918	1.896	39.744	0.342	0.9982	0.9980
		progressive	310.997	5.179	336.769	0.439		
		transient	931.325	208.191	776.948	0.219		
TEST-3	1617.21 s	stationary	374.252	0.950	67.988	0.467	0.9987	0.9985
		progressive	88.412	1.997	536.251	0.382		
		transient	24.393	55.903	1479.750	0.151		
TEST-4	1402.98 s	stationary	253.183	0.985	27.708	0.352	0.9961	0.9956
		progressive	120.585	1.100	429.318	0.444		
		transient	630.454	137.533	721.063	0.204		

Table 4
Best fitting parameters for the Mixed Weibull distribution on the reference damage case with constant H_s and varying GM.

Test	Tmax	Distribution	η	β	γ	w	R^2	R^2_{adj}
TEST-5	1661.53 s	stationary	355.162	1.644	1.001	0.653	0.9983	0.9981
		progressive	229.838	6.955	353.779	0.278		
		transient	109.304	16.361	1500.004	0.069		
TEST-6	2423.21 s	stationary	288.142	1.788	1.000	0.892	0.9980	0.9977
		progressive	142.517	0.702	818.822	0.103		
		transient	46.456	108.267	1123.096	0.005		
TEST-7	2423.68 s	stationary	277.574	1.615	1.000	0.917	0.9981	0.9978
		progressive	140.762	0.802	825.970	0.079		
		transient	430.847	5.270	1020.743	0.004		

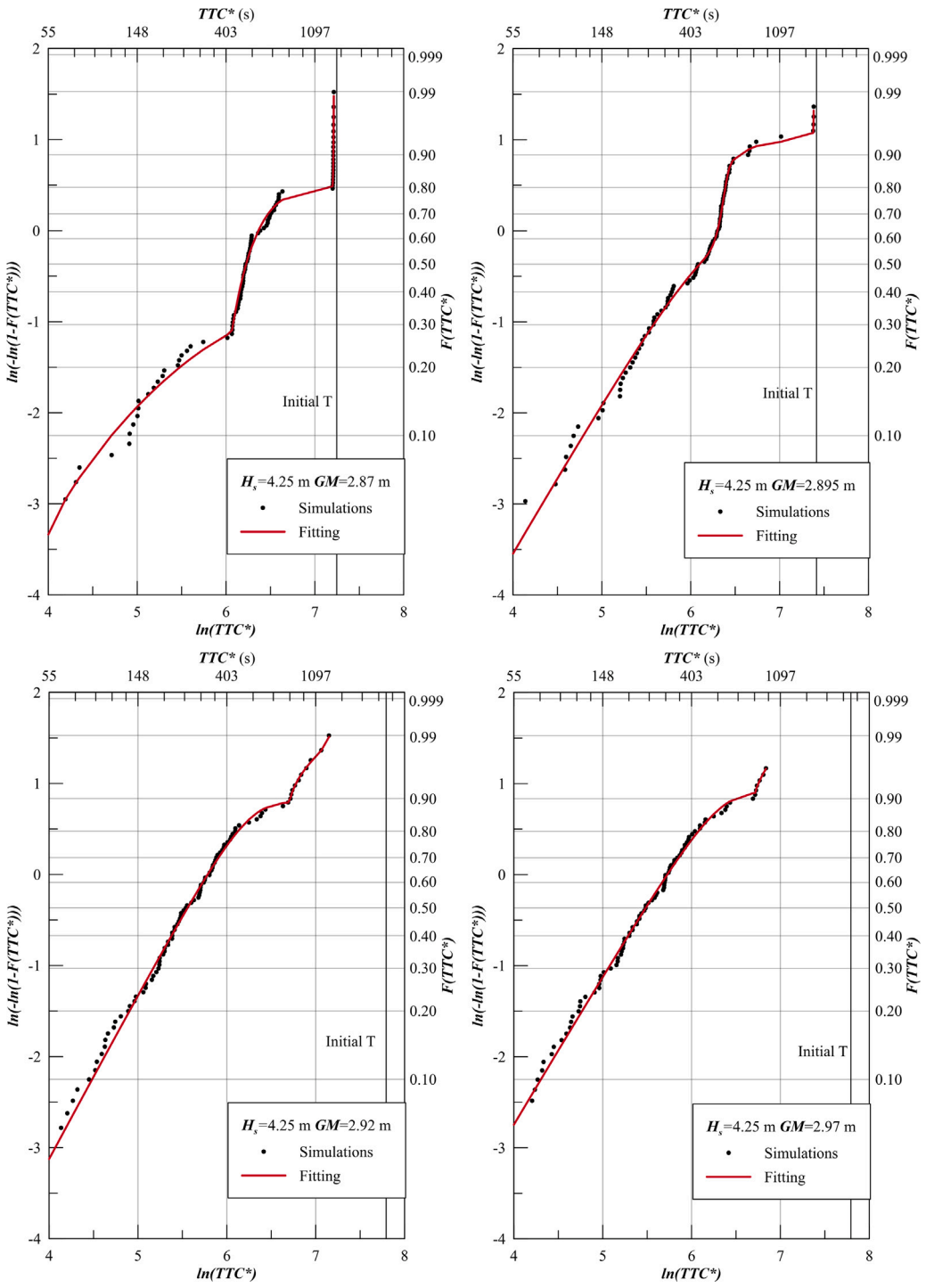

Fig. 8. TTC* cumulative distribution function and Mixed Weibull fitting on the Weibull plot for the reference damage case in TEST-4 (*top-left*), TEST-5 (*top-right*), TEST-6 (*bottom-left*) and TEST-7 (*bottom-right*).

damage stability framework as significant for the damage case. For the tests including transient capsize the value of the mean of 5 repetitions is strongly influenced by the occurrence of a transient event among the 5 tests. In fact there is no monotonic decrease in the time to capsize from TEST-1 to TEST-4 as expected and as predicted by the Mixed Weibull model. The same is for TEST-4 and TEST-5, where a high GM case results in lower TTC. Only the cases without transient capsize (TEST-6 and TEST-7) highlight similar values to the mean of the Mixed Weibull distribution. However, also for those cases, the consideration of the extreme event instead of the mean decreases the TTC of about 800 s, which is impactfull on the evacuation analysis of the ship.

The results highlight variability in the detected shape, scale and location parameter, resulting in different forms for the individual distributions as the condition are changing. However, the number of cases analysed in this paper is too low to permit the detection of a general trend for the coefficients as a function of the GM or the H_s. In fact, possible correlations associated to the analysed breach could be breach-specific as it is, at this stage, impossible to identify a connection between damage and parameter distributions. Therefore, an effective characterisation of the parameters requires further analyses with an extensive set of calculations on critical damage cases identified by a risk analysis framework. As the number of cases analysed in the test is

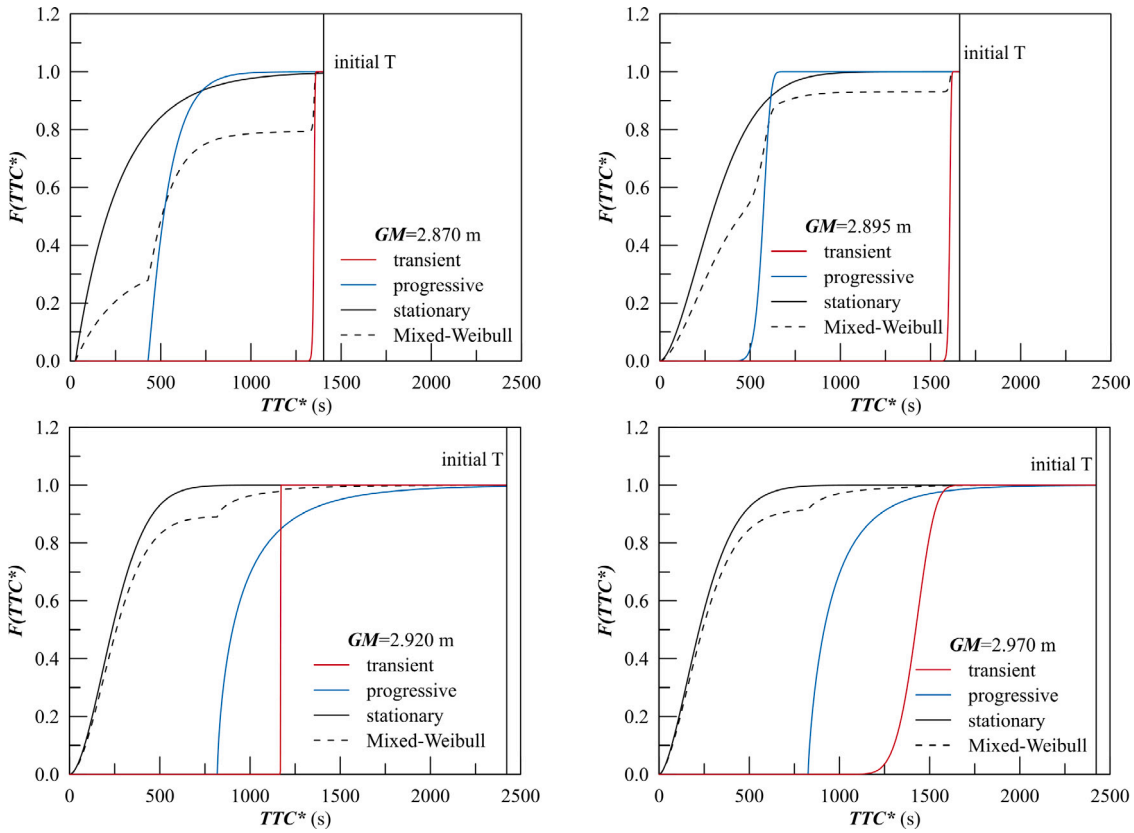

Fig. 9. Cumulative distribution functions for the transient, progressive and stationary capsize for TEST-4 (*top-left*), TEST-5 (*top-right*), TEST-6 (*bottom-left*) and TEST-7 (*bottom-right*).

Table 5
TTC significant values for the provided test cases.

Test	TTC (s)			
	mean first 5 rep.	$p = 0.5$	$p = 0.95$	$p = 0.98$
TEST-1	1164.34	1306.34	56.94	50.11
TEST-2	1373.52	1160.87	51.77	50.05
TEST-3	780.12	1023.01	51.38	48.36
TEST-4	1120.69	900.02	50.25	48.30
TEST-5	958.99	1223.78	61.08	51.95
TEST-6	2482.98	2492.09	1814.34	1576.99
TEST-7	2529.71	2505.77	1840.81	1709.62

not enough to characterise the parameters of the individual distribution in such a way as to identify simpler formulations for the capsize cases, the Mixed-Weibull model represents a good fitting proposal for all the possible capsize modes.

Concerning the time required to estimate the parameters, the differential evolution algorithm takes at most one minute to find a convergent solution, employing a regular laptop without employing parallel programming. Therefore, the computational time for obtaining the analysis is not an issue. The real computational effort is the one needed for running the simulations. In fact, for irregular waves conditions and a complex layout like the provided example, the ratio between the computational time and the time simulated by the calculations is about 1.6. This imply that 100 simulations requires at least 12 h of calculations on a regular laptop, employing 10 parallel processes. For such a reason, the procedure for the estimation should be restricted to critical cases only, properly identified during a flooding risk assessment procedure.

A last comment should be given upon a case that may occur but was is not noticed by the reported test case. All the simulations performed in this paper ends with a capsize event before the maximum time limit of the simulation. However, it may happen that for certain damage cases and environmental conditions the ship will survive at the end of the simulation time. In such cases, the fitting process for the Mixed-Weibull model can be still applied with the consequence that the stationary capsize distribution will have a negative location parameter γ, thus identifying potential capsize cases that may occurs when the TTC is higher than the maximum simulation time t_{max}.

5. Consequences for risk analyses

The characterisation of TTC* (and consequently TTC) through a Mixed-Weibull allows for the opportunity to consider different kinds of significant values for the TTC*, through the direct interpolation of the cumulative curve. As mentioned, it is common practice to use the mean among a few repetitions as a significant value for TTC. Here, instead of the mean, different values can be considered, being representative of the analyses of the extreme, as presented in Table 5. From some of the reported cases, it is evident that a significant part of the capsizes occurs in the transient stage. Thus, this condition is extremely critical for the ship's safety. By considering the mean value of the TTC, leads to a too-optimistic prediction of ship safety.

Such an effect is evident also when the risk of flooding needs to be estimated. In fact, the evaluation of risk through the Potential Loss of Life (PLL) may be strongly influenced by the TTC. By employing a multi-level framework for the evaluation of risk (Vassalos et al., 2023), for the so-called Level-2 prediction, an estimation of the TTC is necessary. In the case of a Level-2.1 prediction, the TTC enters directly into the following empirical formulation for the fatality rate FR determination:

$$FR = \begin{cases} 0.0 & \text{if } TTC > n \\ 0.8\left(1 - \frac{TTC-30}{n-30}\right) & \text{if } 30 \le TTC \le n \\ 1.0 & \text{if } TTC < 30 \end{cases} \tag{14}$$

where n is the maximum allowable evacuation time in minutes according to MSC.1/Circ. 1533.

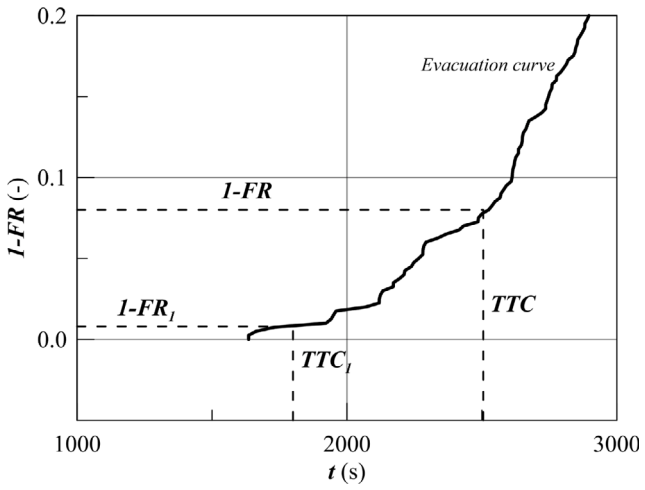

Fig. 10. Fatality rate estimation from different TTC for TEST-7.

In the case of a Level-2.2 prediction, the TTC needs to be directly compared with the evacuation simulations. In such a case, it is of utmost importance that a reliable value of TTC is used, as the TTC is the time threshold necessary to determine the fatality rate of the analysed evacuation scenario.

Therefore, with a flooding scenario that possibly leads to a transient capsize being much more dangerous than others, the sole adoption of the mean value of multiple repetitions as significant to the risk analysis may lead to an underestimation of the risk itself. As an example, for TEST-2, the mean value of TTC is 1,160.87 s, but considering the extreme events with a percentile of 0.98, the significant TTC drops to 50.05 s. With the same assumption, considering TEST-4, the mean value is 900.02 and the 0.98 percentile is 48.30 s. For the cases analysed in this example, a level 2.1 prediction is dependent of the TTC only for TEST-6 and TEST-7, as for the other cases the TTC is lower than 30 min; thus, according to Eq. (14), the fatality rate FR is always equal to 1.0. However, by considering the Level 2.2 prediction, which means a fully direct approach to risk, different TTC led to different fatality rates.

Fig. 10 gives an overview of the process necessary to determine the fatality rate from the evacuation analyses curve. The example refer to a sample evacuation curve for the given scenario (Vassalos et al., 2022b) where the TTC of TEST-7 are employed to evaluate the FR. The reference value is the one for $p = 0.50$ (TTC in the figure) and $p = 0.95$ (TTC_1 in the figure) given in Table 5. The changes in the TTC directly reflects on the $1 - FR$ with a factor 10, going from about 0.080 to 0.008. Thus, changing TTC brings changes in the FR (or $1 - FR$ in the graph). This in turn reflects the PLL evaluation, as the risk is given by the following formulation:

$$PLL = p_f \cdot c_f \tag{15}$$

where p_f is the probability of flooding and c_f identifies the consequences of the associated flooding event. The consequences are evaluated from:

$$c_f = FR \cdot POB \tag{16}$$

where FR is the fatality rate and POB is the number of people onboard. As such, the FR is directly influenced by the reference value for the TTC as highlighted by Fig. 10, reflecting its consequences on the risk assessment of a passenger ship in a modern damage stability framework. The possibility to evaluate in a more appropriate way the TTC for critical cases is for sure an added value compared to the standard assumptions used in damage stability. Moreover, the methodology based on the Mixed Weibull distributions enlarges the importance of first principle method to study the flooding risk for passenger ships.

6. Conclusions

The present paper proposes a novel methodology to determine the statistics of Time to Capsize of a damaged ship by applying the extreme value theorem. A Mixed-Weibull model is introduced to capture the three different capsize modes: transient, progressive, and stationary.

Thanks to the application of an evolutionary algorithm, it is possible to automatically fit the 12 parameters needed to characterise the Mixed-Weibull regression model. The provided regressions on seven reference cases highlight considerably high goodness of fit, evaluated through both R^2 and R^2_{adj} parameters. Furthermore, the differential evolution algorithm directly assign the weights of single sub-populations, allowing for recognising cases where only 2 sub-populations are predominant as for the cases with higher GM values.

The reference cases have been tested with 100 repetitions per case to capture the random nature of irregular waves. This is a completely different methodology of estimating TTC, namely, employing the mean of 5 repetitions only. As the number of calculations is significantly high, taking into consideration the amount of time needed to perform a calculation, it is not advisable to perform such a detailed analysis for all the cases being analysed within a damage stability framework, but only on a reduced set of critical cases, in such a way as to inform a forensic analysis of the case itself.

The provided methodology highlights conditions between the repetitions that are potentially dangerous for the vessel, as a transient capsize case may still occur whilst progressive or stationary stage are detected for other repetitions, something that the conventional methods do not detect as only the mean of five repetitions is considered. In addition, it should be specified that the simulations where performed setting all the openings to be opened. The eventual consideration of leaking and collapsing closed non-watertight doors may be further influence the TTC, something that should be investigated in dedicated studies on the topic.

Furthermore, being able to characterise the TTC by means of a mixed distribution may allow for future studies aiming at a fully probabilistic estimation of loss of life after an accident, which means convolute the distribution of the time to capsize with the distribution of the time to evacuate obtained by evacuation analyses.

CRediT authorship contribution statement

Francesco Mauro: Writing – review & editing, Writing – original draft, Visualization, Validation, Software, Methodology, Investigation, Formal analysis, Data curation, Conceptualization. **Dracos Vassalos:** Writing – review & editing, Supervision.

Declaration of competing interest

The authors declare that they have no known competing financial interests or personal relationships that could have appeared to influence the work reported in this paper.

Data availability

Data will be made available on request.

References

Berliant, J., Teugels, J., Vynkier, F., 1996. Practical Analysis of Extreme Values. Leuven University Press.

Bulian, G., Cardinale, M., Dafermos, G., Lindroth, D., Ruponen, P., Zaraphonitis, G., 2020. Probabilistic assessment of damaged survivability of passenger ships in case of grounding or contact. Ocean Eng. 218, 107396.

Cichowicz, J., Tsakalakis, N., Vassalos, D., Jasionowski, A., 2016. Damage survivability of passenger ships - re-engineering the safety factor. Safety 2 (4), 1–18.

FLARE, 2022. Flooding Accident Response. Technical Report, Horizon 2020 Project 2019-2022.

FLOODSTAND, 2012. Integrated Flooding Control and Standard for Stability and Crisis Management. Technical Report, FP7 - DG Research project.

GOALDS, 2012. GOAL Based Damage Stability. Technical Report, EU-funded research project.

Guarin, L., Murphy, A., Vassalos, D., Paterson, D., Mauro, F., Boulougouris, E., 2021. D5.4 Dynamic Vulnerability Screening. Technical Report, Project FLARE.

Hasselmann, K., Olbers, D., 1973. Measurements of wind-wave growth and swell decay during the Joint North Sea Wave Project (JONSWAP). Ergänzung zur Deut. Hydrogr. Z. 8 (12), 1–95.

IMO, 2022. International Convention for the Safety of Life at Sea (SOLAS). Technical Report, International Maritime Organisation, Consolidated edition as of 2022.

Jasionowski, A., 2001. An Integrated Approach to Damage Ship Survivability Assessment (Ph.D. thesis). University of Strathclyde.

Luhmann, H., Bulian, G., Vassalos, D., Olufsen, O., Seglem, I., Pottgen, J., 2018. eSAFE-D4.3.2 - Executive Summary. Technical Report, Joint Industry Project eSAFE - enhanced Stability After a Flooding Event - A joint industry project on Damage Stability for Cruise Ship.

Mallipeddi, R., Suganthan, P.N., Pan, Q.K., Tasgetiren, M.F., 2011. Differential evolution algorithm with ensemble of parameters and mutation strategies. Appl. Soft. Comput. 11, 1679–1696.

Mauro, F., Nabergoj, R., 2017. An enhanced method for extreme loads analysis. Brodogradnja 68 (2), 79–93.

Mauro, F., Vassalos, D., Paterson, D., 2022a. Critical damages identification in a multi-level damage stability assessment framework for passenger ships. Reliab. Eng. Syst. Saf. 228, 108802.

Mauro, F., Vassalos, D., Paterson, D., Boulougouris, E., 2022b. Exploring smart methodologies for critical flooding scenarios detection in the damage stability assessment of passenger ships. Ocean Eng. 262, 112289.

Mauro, F., Vassalos, D., Paterson, D., Boulougouris, E., 2023. Evolution of ship damage stability assessment - Transitioning designers to direct numerical simulations. Ocean Eng. 268, 113387.

Ruponen, P., Valanto, P., Acanfora, M., Dankowski, H., Lee, G.J., Mauro, F., Murphy, A., Rosano, G., van't Veer, R., 2022a. Results of an international benchmark study on numerical simulation of flooding and motions of a damaged ropax ship. Appl. Ocean Res. 123, 103153.

Ruponen, P., van Basten-Batemburg, R., van't Veer, R., Bu, S., Dankowski, H., Lee, G., Mauro, F., Ruth, E., Tompuri, M., 2022b. International benchmark study on numerical simulation of flooding and motions of a damaged cruise ship. Appl. Ocean Res. 129, 103403.

Spanos, D., Papanikolaou, A., 2014. On the time for abandonment of flooded passenger ships due to collision damages. J. Mar. Sci. Technol. 19, 317–327.

Storn, R., Prince, K., 1997. Differential evolution - a simple and efficient heuristic for global optimization over continuous spaces. J. Global Optim. 11, 341–359.

Vassalos, D., 2022. The role of damaged ship dynamics in addressing the risk of flooding. Ship Offshore Struct. 17 (2), 279–303.

Vassalos, D., Paterson, D., 2021. Towards unsinkable ships. Ocean Eng. 232, 109096.

Vassalos, D., Paterson, D., Mauro, F., 2023. Real-time flooding risk evaluation for ship-to-ship collisions based on first principles. Ocean Eng. 281, 114847.

Vassalos, D., Paterson, D., Mauro, F., Mujeeb-Ahmed, M., Boulougouris, E., 2022a. Process, methods and tools for ship damage stability and flooding risk assessment. Ocean Eng. 266, 113062.

Vassalos, D., Paterson, D., Mauro, F., Murphy, A., Mujeeb-Ahmed, M., Michalec, R., Boulougouris, E., 2022b. A multi-level approach to flooding risk estimation on passenger ships. In: Proceedings of SNAME 14th International Marine Design Conference IMDC. IMDC, Vancouver, BC, Canada.